JOURNAL

OF THE AMERICAN CHEMICAL SOCIETY

© Copyright 1986 by the American Chemical Society

VOLUME 108, NUMBER 17 AUGUST 20, 1986

Theoretical Study of the Uncatalyzed Hydration of Carbon Dioxide in the Gas Phase

Jiin-Yun Liang and William N. Lipscomb*

Contribution from Gibbs Chemical Laboratories, Department of Chemistry, Harvard University, Cambridge, Massachusetts 02138. *Received December 16, 1985*

Abstract: The reaction energy surface and pathway of the reversible gas-phase reaction of CO_2 with H_2O and OH^- have been evaluated with PRDDO and 4-31G SCF-MO methods, including one MP2 correlation calculation. In the most favorable pathway, H and O of water approach respectively O and C of CO_2 simultaneously, and after the transition state is passed the new OH bond is formed followed by formation of the new CO bond. The major components of the energy barrier are analyzed, and the ways to lower the energy barrier are discussed. The deformation energies of CO_2 and H_2O contribute most to the barrier, and the exchange repulsive interactions are also important. After corrections for zero-point vibrational energies and thermal energies and inclusion of entropic effects, the free energy barrier of the hydration reaction is about 62 kcal/mol at the 4-31G level, 64.6 kcal/mol at the 4-31G+ level, and about 60.7 kcal/mol when 4-31G**/MP2 correlation corrections are made at the 4-31G geometry. Entropic changes, included in these values, contribute some 15% to the activation free energy. A population analysis indicates locations of charges which may be stabilized by external charges in hydration and catalysis. For dehydration of H_2CO_3 the barrier arises primarily from loss of interaction energies which can be described as charge transfer and electrostatic interactions. For the reaction of CO_2 with OH^- no barrier is found; here the deformation energy for CO_2 is smaller than the charge transfer and electrostatic interactions as CO_2 and OH^- react, owing to the extra negative charge on OH^-. The sequences of electron flow in these reactions are described in terms of localized orbitals.

In aqueous solution in the absence of carbonic anhydrase the reactions[1]

$$H_2O + CO_2 \underset{20\ s^{-1}}{\overset{0.035\ s^{-1}}{\rightleftharpoons}} H_2CO_3 \qquad (1)$$

$$OH^- + CO_2 \underset{2\times10^{-4}\ s^{-1}}{\overset{8500\ s^{-1}\ M^{-1}}{\rightleftharpoons}} HCO_3^- \qquad (2)$$

have activation energies of 17.7 (forward) and 14.6 kcal/mol (reverse) for reaction 1[2] and 13.1 kcal/mol for the forward direction of reaction 2.[3] Human carbonic anhydrase C (HCAC) catalyzes the reaction

$$H_2O + CO_2 \underset{}{\overset{6\times10^5\ s^{-1}}{\rightleftharpoons}} HCO_3^- + H^+ \qquad (3)$$

at rates which are faster than the uncatalyzed reaction by a factor of about 10^7. If all of this rate enhancement enters the activation energy, the enzyme reduces the barrier by about 10 kcal/mol, assuming little or no barrier to proton transfer. It is now widely accepted that the enzymic reaction is catalyzed by Zn^{+2}-bound hydroxide ion, and the proton transfer is catalyzed by a non-Zn^{+2}-liganded histidine and by buffer in HCAC.[4-8]

The gas-phase reactions of carbon dioxide with water and with hydroxide ion have been studied earlier by others,[9-12] focusing mainly on accurate reaction energies. Further investigations of the reaction on properties such as the most important energetic components to the reaction barriers, the redistribution of the charges, the sequences of bond formation and cleavage, and the thermodynamic properties of the reaction at room temperature are, however, lacking.

We consider here the nonenzymic, gas-phase reactions of carbon dioxide with water and with hydroxide ion, which we show to have calculated free energy barriers of 61 kcal/mol and 0, respectively. In addition, we establish a two-dimensional energy surface from which we find the most favorable reaction pathway (MFRP) using the PRDDO (minimum basis) method.[13,14] Structures of the complex along the MFRP are optimized at the 4-31G SCF-MO level. We then make an analysis of (a) deformation energies and interaction energies of the reactants in order to understand the major energetic components, (b) localized molecular orbitals (LMO) along the MFRP in order to describe sequentially bond

(1) Kern, D. M. *J. Chem. Educ.* **1960**, *37*, 14.
(2) Magid, E.; Turbeck, B. O. *Biochim. Biophys. Acta* **1968**, *165*, 515.
(3) Pinsent, B. R. W.; Pearson, L.; Roughton, F. J. W. *Trans. Faraday Soc.*, **1956**, *52*, 1512.
(4) Lindskog, S. In *Zinc Enzymes*; Spiro, T. G., Ed.; John Wiley & Sons: New York, 1983; p 77.
(5) Pocker, Y.; Sarkanen, S. *Adv. Enzymol.* **1978**, *47*, 149.
(6) Prince, R. H. *Adv. Inorg. Chem. Radiochem.* **1979**, *22*, 349.
(7) *Biophysics and Physiology of Carbon Dioxide*; Bauer, C., Gros, G., Bartels, H., Eds.; Springer-Verlag: New York, 1980.
(8) Lipscomb, W. N. *Annu. Rev. Biochem.* **1983**, *52*, 17.
(9) (a) Jönsson, B.; Karlström, G.; Wennerström, H.; Forsen, S., Roos, B. Almlof, J. *J. Am. Chem. Soc.* **1977**, *99*, 4628. (b) Jönsson, B.; Karlström, G.; Wennerström, H. *Chem. Phys. Lett.* **1976**, *41*, 317.
(10) Jönsson, B.; Karlström, G.; Wennerström, H. *J. Am. Chem. Soc.* **1978**, *100*, 1658.
(11) Nguyen, M. T.; Ha, T. K. *J. Am. Chem. Soc.* **1984**, *106*, 599.
(12) Williams, J. O.; van Alsenoy, C.; Schafer, L. *J. Mol. Struct.* **1981**, *76*, 109.
(13) Halgren, T. A.; Lipscomb, W. N. *J. Chem. Phys.* **1973**, *58*, 1569.
(14) Marynick, D. S.; Lipscomb, W. N. *Proc. Natl. Acad. Sci. U.S.A.* **1982**, *79*, 1341.

0002-7863/86/1508-5051$01.50/0 © 1986 American Chemical Society

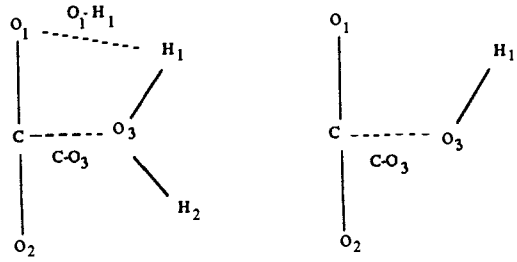

Figure 1. The two reaction coordinates of reaction 1 are C–O_3 and O_1–H_1, and the one for reaction 2 is C–O_3.

formation and bond cleavage, and (c) geometry and Mulliken population in order to study charge redistribution along the MFRP. A comparison is made of this analysis for reactions 1 and 2. The thermodynamic properties of these reactions are considered briefly in the Discussion and so is the possible stabilization of the transition state by the enzyme.

Methods

(1) Basis Sets. PRDDO,[13,14] based on partial retention of diatomic differential overlap over an orthogonalized basis, is an approximation to the LCAO–SCF calculations at the minimum basis set level. It retains one-, two-, and three-center integrals of the form $(X_{ia}X_{jb}|X_{kc}^2)$, where X_{ia} is a symmetrically orthogonalized AO mainly centered on the atom a. Also retained are one- and two-center exchange integrals of the form $(X_{ia}X_{ja}|X_{ia}X_{ja})$ and $(X_{ia}X_{ja}|X_{ia}X_{jb})$. Problems of rotational invariance are avoided by choice of local axes which are unique in anisotropic environments. Retention of $\sim N^3$ integrals in PRDDO is shown to simulate efficiently the STO-3G SCF results.[15] We also employ the Gaussian 82 program using the 4-31G basis[16] of Pople and the 4-31G+ basis[17] obtained by adding sp-type diffuse orbitals (with exponents 0.04 for C and 0.068 for O) on the heavy atoms in 4-31G. A few calculations with 4-31G**[18] are also included, and correlation corrections are obtained by Møller–Plesset perturbations[19] of the 4-31G** wave function to second order (MP2).

(2) Energy Surface. We assume that CO_2 and H_2O remain coplanar in the reaction. (The van der Waals complex is predicted to be coplanar with C–O_3 about 2.63 Å.[20]) Our two reaction coordinates are C–O_3 and O_1–H_1 (Figure 1). Using PRDDO we optimized geometries at each of 216 selected points within 1.37 Å < C–O_3 < 2.7 Å and 0.99 Å < O_1–H_1 < 3.2 Å. The average interval between nearest points is 0.1 Å, although this interval is less around the MFRP.

(3) The Most Favorable Reaction Pathway (MFRP). The MFRP is then traced on the energy surface starting from reactants (upper right, Table I and Figure 2) and advancing along the smaller energy increase either downward or leftward toward the transition state. This method will locate the transition state if the step size is sufficiently small. The molecular structures along this MFRP are further optimized at the 4-31G SCF–MO level with Gaussian 82.[16]

(4) Energy Analysis. The energy changes of a reacting complex at a point along the reaction pathway can be written, following Kitaura and Morokuma,[21-23] as

$$\Delta E = E_{\text{complex}} - E_{\text{isolated reactants}}$$

$$\Delta E = \Delta E_{\text{DEF}} + \Delta E_{\text{INT}}$$

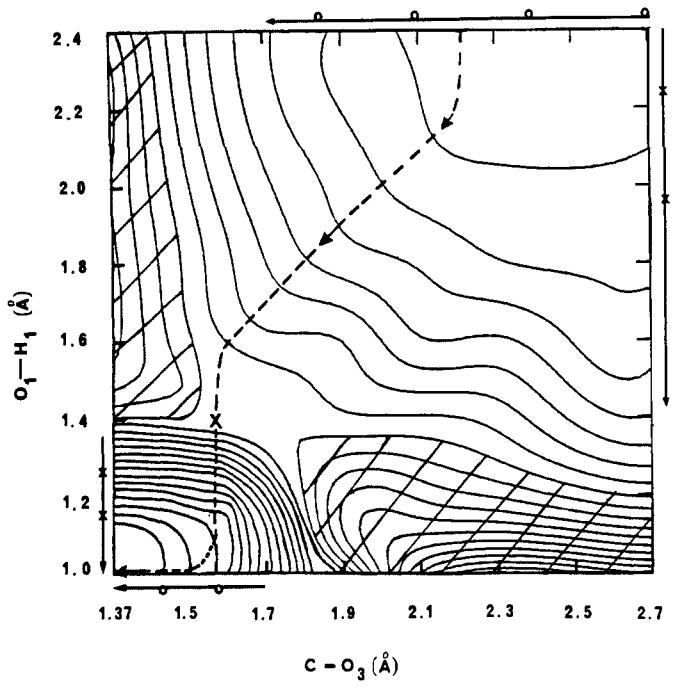

Figure 2. The energy surface for reaction 1. The contour is obtained by a two-dimensional spline on the data listed in Table I. The energy interval between nearest curves is 5 kcal/mol. The MFRP is traced as a dashed line and the transition state by a sign ×. If only C–O_3 or O_1–H_1 is chosen as reaction coordinate a discontinuous jump in the other coordinate would be required, as indicated by o or x along the border.

where ΔE is the total reaction energy, ΔE_{DEF} is the deformation energy of the reactants

$$\Delta E_{\text{DEF}} = E_{\text{deformed reactants}} - E_{\text{isolated reactants}}$$

and ΔE_{INT} is the interaction energy between the deformed reactants

$$\Delta E_{\text{INT}} = E_{\text{complex}} - E_{\text{deformed reactants}}$$

Furthermore, the total interaction energy ΔE_{INT} can be decomposed into contributions from the electrostatic interaction, ΔE_{ES}, exchange interaction, ΔE_{EX}, polarization interaction, ΔE_{PL}, charge-transfer interaction (delocalization), ΔE_{CT}, and coupling terms between the various energy components, ΔE_{MIX}.

Results

(1) Reaction 1. The energy surface (Table I) contains energies relative to the sum of energies of the reactants. The saddle point (Figure 2) is at 1.575 Å for C–O_3 and 1.4 Å for O_1–H_1. Shaded areas are higher (less stable) and unshaded areas are lower (more stable) energies relative to the saddle point energy. In the upper right (Figure 2) the unshaded area contains pathways in which H_2O can have many relative orientations as it approaches CO_2. At the PRDDO level the forward and reverse directions have barriers of ~33 and ~74 kcal/mol, respectively. The MFRP is indicated by the path of arrows in Table I and by a dashed line in Figure 2. Above 1.6 Å the reaction is concerted, with C–O_3 about equal to O_1–H_1. After the saddle point (see above), O_1–H_1 reduces to 0.99 Å while C–O_3 remains at about 1.575 Å after which C–O_3 reduces to 1.367 Å. These PRDDO structures yield new energies after the MFRP is optimized at the 4-31G level. Unless stated otherwise the analysis below refers to the MFRP obtained from these 4-31G calculations.

An overall view of the relative energies of reactants, transition state, and product is shown on Table II. The stability of H_2CO_3 relative to H_2O and CO_2 at the 4-31G level is barely reversed at the 4-31G** (polarization functions on all atoms) level and de-

(15) Scheiner, S.; Lipscomb, W. N.; Kleier, D. A. *J. Am. Chem. Soc.* **1976**, *98*, 4770.
(16) Ditchfield, R.; Hehre, W. J.; Pople, J. A. *J. Chem. Phys.* **1971**, *54*, 724.
(17) Clark, T.; Chandrasekhar, J.; Spitznagel, G. W.; von Ragué Schleyer, P. *J. Comp. Chem.* **1983**, *4*, 294.
(18) Hariharan, P. C.; Pople, J. A. *Theor. Chim. Acta* **1973**, *28*, 213.
(19) Møller, C.; Plesset, M. S. *Phys. Rev.* **1934**, *46*, 618.
(20) Jönsson, B.; Karlström, G.; Wennerström, H. *Chem. Phys. Lett.* **1975**, *30*, 58.
(21) Morokuma, K. *J. Chem. Phys.* **1971**, *55*, 1236.
(22) Kitaura, K.; Morokuma, K. *Int. J. Quantum Chem.* **1976**, *10*, 325.
(23) Morokuma, K.; Kitaura, K. In *Molecular Interactions*; Ratajczak, H., Orville-Thomas, W. J., Eds.; John Wiley & Son: New York, 1980; Vol. 1.

Table I. PRDDO Energy Surface of Reaction 1 (Energy in kcal/mol)[a]

O_1–H_1 (Å)	C–O_3 (Å)																		
	1.37	1.4	1.5	1.55	1.575	1.6	1.65	1.7	1.8	1.9	2.0	2.1	2.2	2.3	2.4	2.5	2.6	2.7
3.2			43.8					15.4		3.5		-1.2	-4.8	-5.0	-5.4	-5.3	-5.2	-4.8
3.1														-5.4	-5.4	-4.9	-5.1	
3.0	-10.0		32.2					11.8		3.6		-1.2	-4.1	-5.6	-5.5	-5.4	-5.0	-4.6
2.9														-5.3	-5.3	-5.6	-5.4	
2.8	52.5		29.4					13.9		1.9		-2.6	-4.8	-5.5	-5.8	-5.5	-5.5	-4.0
2.7														-5.6	-5.6	-5.5	-5.2	
2.6	47.8		24.7					9.5		2.1		-3.3	-4.8	-5.5 ←	-5.7	-5.3		-4.2
2.5													-4.9 ←	-5.0	-4.7	-5.0		
2.4	45.8		23.7					9.5		2.7		-2.6	-3.9	-4.6	-4.9	-4.5		-3.2
2.2	50.6		25.7					10.9		3.5		-1.2	-3.0	-3.3		-3.2		-2.5
2.1											2.1	-0.4 ←	-1.8	-2.2				
2.0	48.6		29.0					14.5		7.0	3.9 ←	1.3	0.0	-0.6		-0.8		-0.3
1.9									11.6	8.5 ←	5.9	4.0						
1.8	50.0		31.9					18.6	14.0 ←	11.3	8.6	8.1	7.6	4.0		2.9		2.4
1.7	50.3		33.3			26.1 ←	23.8 ←	21.1 ←	17.9	14.8		11.6		10.4		4.9		4.1
1.6	50.0	44.8	34.3	31.6	29.9 ←	28.8	26.4	25.0	21.8	23.5		14.1		14.3		8.2		6.5
1.55	48.3		34.9	32.1	31.0	30.3	28.4											
1.5		38.0	35.0	33.7	32.6	31.3	30.1	29.8				23.1						
1.45			34.9	33.1	32.5	32.3	32.3											
1.425				33.1	32.7	32.5												
1.4	32.9	33.0	33.9	33.3	32.9	32.7	34.3	34.2		29.7		29.2	32.5	26.4		17.5		13.7
1.375				32.7	32.8	33.0												
1.35			30.7	31.8	32.5	33.0	35.1	34.5										
1.3	-2.6	-2.2	8.1	29.1	30.3	31.8		36.0										
1.2	-20.7	-20.4	-9.9	-7.1	-3.6	-0.3		16.7		48.1		46.9		42.2		36.3		32.2
1.1	-34.8	-34.4	-26.7	-21.1	-17.8	-14.3		1.9		39.0		65.6						
0.99	-41.4 ←	-41.1 ←	-30.5 ←	-27.8 ←	-24.6	-21.0		-3.6		32.7		73.8		87.6		83.8		78.2

[a] The energies listed here are relative to the combined energy of the isolated molecules CO_2 and H_2O.

Table II. Relative Energies of Reaction 1[a]

	species		
	$H_2O + CO_2$	TS	H_2CO_3
4-31G	0.0	53.4	−4.8
4-31G**	0.0	63.5	1.3
4-31G**/MP2	0.0	52.5	6.1
4-31G+	0.0	56.1	−2.3
4-31G+/MP2	0.0	56.5	13.1
ΔH	0.0	51.9 (54.9)	−1.7 (1.1)
ΔS	0.0	−32.2 (−32.5)	−33.4 (−33.5)
ΔG	0.0	61.5 (64.6)	8.3 (11.1)

[a] Energies are in kcal/mol and entropies in cal/(mol·K). Results of ΔH, ΔS, and ΔG at 298 K are from both 4-31G and 4-31G† (in parentheses) calculations.

cisively reversed when correlation is added at the MP2 level. The energy of the transition state relative to the energies of the reactants increases by 10 kcal/mol when polarization functions are included and decreases to 52.5 kcal/mol when correlation is included (Table II). Furthermore, we find that the 4-31G+ basis and the 4-31G basis yield similar results and that the 4-31G+/MP2 basis reverses the stability of H_2CO_3 relative to H_2O and CO_2 (Table II).

The energy analysis includes deformation energies, $\Delta E_{DEF}(CO_2)$ and $\Delta E_{DEF}(H_2O)$, for CO_2–H_2O complex along the MFRP (Table III). For CO_2, $\Delta E_{DEF}(CO_2)$ increases from 3.7 kcal/mol at C–O_3 = O_1–H_1 = 2.0 Å to 74.3 kcal/mol in the product. This deformation energy is correlated with the angle O_1–C–O_2 (correlation coefficient −0.982) and is mostly associated with repulsions between electrons around O_1 and O_2 as well as with decreased bonding between C and O. The deformation energy of H_2O correlates with the angle H_1–O_3–H_2 (coefficient 0.94) and increases from 0.5 kcal/mol at C–O_3 = O_1–H_1 = 2.0 Å, to 29.2 kcal/mol at the transition state, and to ~200 kcal/mol after the reaction crosses the transition state and the O_3–H_1 bond breaks. Our analysis also includes the interaction energy between CO_2 and H_2O, ΔE_{INT}, which increases from 1.3 kcal/mol at C–O_3 = O_1–H_1 = 2.0 Å to 16 kcal/mol at C–O_3 = 1.6 Å and O_1–H_1 = 1.5 Å. After the transition state is passed large negative interactions occur. At the transition state $\Delta E_{DEF}(CO_2)$ at 25.7 kcal/mol and $\Delta E_{DEF}(H_2O)$ at 29.2 kcal/mol are the most important contributions to the barrier of the hydration reaction. On the other hand, the barrier in the dehydration reaction arises mainly from the loss of interaction energy. The interaction components (charge transfer, polarization, and electrostatic interactions) remain negative throughout the reaction, and their magnitudes increase as hydration proceeds (Table IV). These negative components are more than cancelled by the positive exchange interactions and partly by coupling terms. Before the transition state is reached (hydration direction) the stabilizing interactions (Table IV) are $\Delta E_{ES} > \Delta E_{CT} > \Delta E_{PL}$, while charge transfer dominates the post transition states. Large coupling occurs between the charge transfer and polarization interactions.[24]

Localized orbitals, obtained by the method of Boys,[25] show the sequence of electron flow in the reaction. Each bond in Figure 3 represents a localized orbital derived from the SCF wave function which, we stress, is consistent with the exclusion principle. The appearance of more than four bonds to carbon or oxygen (counting lone pairs) is thus due to fractional use of atomic orbitals in these localized bonds. The partly concurrent four steps of Figure 3 are analyzed as (a)...(d) as follows.

(a) One C–O_1 bonding orbital is induced by the lone pairs of the H_2O molecule to change to a lone pair on O_1 as C–O_3 = O_1–H_1 changes from 1.8 to 1.7 Å. For this change ΔE is 9.5 kcal/mol, and the CO_2 becomes bent. While there are also repulsive interactions of the lone pairs of H_2O with bonding orbitals of C–O_2, they are much weaker, because of the orientation assumed here. In the electron redistribution, electrons move from C, H_1, and H_2 to O_1, O_2, and O_3. Atom O_1 receives most of the negative charge (ΔQ = −0.032) and H_1 becomes slightly more positive (ΔQ = 0.023).

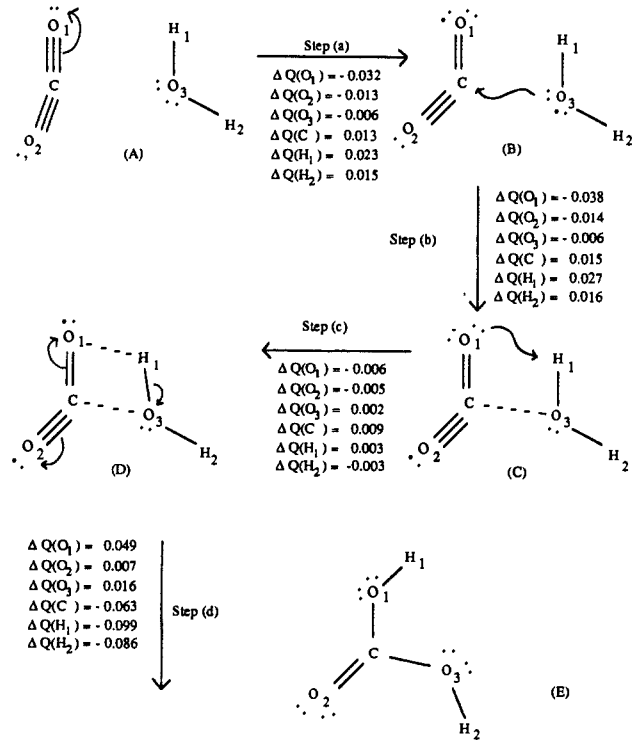

Figure 3. A sequential picture of electron flow for reacton 1 based on localized molecular orbitals. Step a: One C–O_1 bonding orbital changes to a lone pair on O_1 as C–O_3 = O_1–H_1 changes from 1.8 to 1.7 Å. Step b: Nucleophilic attack from O_3 to C as C–O_3 = O_1–H_1 changes from 1.7 to 1.6 Å. Step c: A lone pair on O_1 develops to form O_1–H_1 bonding orbital as C–O_3 = 1.6 Å and O_1–H_1 = 1.4 Å changes to C–O_3 = 1.575 Å and O_1–H_1 = 1.4 Å. Step d: A concerted transformation of bonding orbitals C–O_1, C–O_2, and O_3–H_1 to lone pairs on O_1, O_2, and O_3, respectively, as C–O_3 = 1.575 Å and O_1–H_1 = 1.35 Å changes to C–O_3 = 1.575 Å and O_1–H_1 = 1.3 Å. Because of fractional utilization of atomic orbitals in these LMOs, the exclusion principle is not violated when more than four "bonds" and/or electron pairs are shown at an atomic center.

(b) Nucleophilic attact from O_3 to C becomes substantial as C–O_3 = O_1–H_1 changes from 1.7 to 1.6 Å. For step b, ΔE is 10.9 kcal/mol. Further movement of electrons from C, H_1, and H_2 to O_1, O_2, and O_3 occurs, with additional increments of −0.038 to O_1 and 0.027 (electron loss) on H_1. Although O_3 attacks, it gains electrons slightly (ΔQ = −0.006) from H_1 and H_2.

(c) A lone pair on O_1 develops O_1–H_1 bonding as C–O_3 = 1.6 Å and O_1–H_1 = 1.4 Å change to C–O_3 = 1.575 Å and O_1–H_1 = 1.4 Å. For step c, ΔE is 1.1 kcal/mol. The formation of the O_1–H_1 bond is facilitated by the sum of charge increments in steps a and b of −0.07 on O_1 and 0.05 on H_1.

(d) A concerted reaction occurs between the transition state C–O_3 = 1.575 Å and O_1–H_1 = 1.35 Å to C–O_3 = 1.575 Å and O_1–H_1 = 1.3 Å, for which ΔE = −5.4 kcal/mol. Localized bonding orbitals C–O_1, C–O_2, and O_3–H_1 transform to lone pairs on O_1, O_2, and O_3, respectively, accompanied by other geometry changes toward the product H_2CO_3. Electrons finally flow back from O_1, O_2, and O_3 to the original donors C, H_1, and H_2.

Two molecular orbitals bond all four atoms C, O_1, H_1, and O_3 in structure D (Figure 3). The PRDDO pathway is similar to that described above for the 4-31G method, except that the concerted reaction of step d becomes two steps, the first of which is that the C–O_2 bond becomes a lone pair on O_2 and the second is the other part of step d as shown in Figure 3.

Geometric and population analyses (Table V) show the expected negative correlations between bond lengths and bond orders. For example, C–O_1 and C–O_2 lengthen as electron density is lost to form O_1–H_1 and C–O_3. Stabilization of the transition state relative

(24) Nagase, S.; Fueno, T.; Yamabe. S.; Kitaura, K. *Theor. Chim. Acta (Berlin)* **1978**, *49*, 309.
(25) Boys, S. F. *Rev. Mod. Phys.* **1960**, *32*, 296.

Table III. Energy Analysis of Reaction 1 (4-31G)

reaction coord (Å)		energy[a] (kcal/mol)				angle (deg)	
$C-O_3$	O_1-H_1	$\Delta E_{DEF}(CO_2)$	$\Delta E_{DEF}(H_2O)$	$\Delta E(CO_2-H_2O)$	ΔE_{INT}	$\angle O_1-C-O_2$	$\angle H_1-O_3-H_2$
1.349	0.953	74.3	204.5	-4.8	-283.6	124.7	173.4
1.575	1.3	58.6	202.3	48.0	-212.9	130.8	176.4
1.575	1.35	25.7	29.2	53.4	-1.5	147.3	143.4
1.575	1.4	23.3	19.3	51.5	8.9	148.3	139.2
1.6	1.4	21.3	17.3	50.4	11.9	149.5	137.9
1.6	1.5	19.3	9.8	45.0	15.9	150.2	137.9
1.6	1.6	18.5	6.4	40.0	15.1	150.4	129.8
1.7	1.7	12.7	3.2	29.1	13.2	154.5	124.8
1.8	1.8	8.6	1.6	19.6	9.4	158.4	121.0
1.9	1.9	5.7	0.8	11.9	5.4	162.1	118.4
2.0	2.0	3.7	0.5	5.5	1.3	165.4	116.5

[a] $\Delta E_{DEF}(CO_2)$: deformation energy of CO_2, relative to isolated CO_2. $\Delta E_{DEF}(H_2O)$: deformation energy of H_2O, relative to isolated H_2O. $\Delta E(CO_2-H_2O)$: total reaction energy of CO_2-H_2O complex relative to the sum of energies of CO_2 and H_2O. ΔE_{INT}: interaction energy between deformed CO_2 and H_2O.

Table IV. Interaction Components in Reaction 1 (4-31G)

reaction coord (Å)		interaction energies[c] (kcal/mol)						charges transferred
$C-O_3$	O_1-H_1	ΔE_{INT}	ΔE_{MIX}	ΔE_{EX}	ΔE_{PL}	ΔE_{ES}	ΔE_{CT}	$Q(CT)$[d]
1.575	1.3	-212.9[b]	-108.8	308.1	-70.8	-155.4	-186.1	0.37
1.575	1.35[a]	-1.5	51.2	267.9	-58.7	-145.0	-116.9	0.15
1.575	1.4	8.9	57.3	257.6	-59.6	-138.9	-107.6	0.16
1.6	1.4	11.9	50.7	240.9	-52.5	-129.2	-98.0	0.15
1.6	1.5	15.9	51.1	223.7	-51.0	-122.4	-85.6	0.16
1.6	1.6	15.1	48.7	210.8	-48.6	-118.2	-77.6	0.16
1.7	1.7	13.2	23.8	148.1	-26.0	-86.1	-46.6	0.12
1.8	1.8	9.4	11.2	103.7	-14.0	-63.4	-28.1	0.09
1.9	1.9	5.4	5.2	72.4	-7.9	-47.1	-17.2	0.06
2.0	2.0	1.3	2.4	50.3	-4.7	-35.9	-10.8	0.05

[a] Transition state: $C-O_3$ = 1.575 Å, O_1-H_1 = 1.35 Å. [b] The geometry changes substantially between the first and second lines (step d in Figure 3). [c] ΔE_{INT}: total interaction energy between deformed CO_2 and H_2O. ΔE_{MIX}: the coupling term between various interactions. ΔE_{EX}: exchange interaction. ΔE_{CT}: charge-transfer interaction. ΔE_{PL}: polarization interaction. ΔE_{ES}: electrostatic interaction. [d] $Q(CT)$: charge (in electron) transferred from H_2O to CO_2.

Table V. Atomic Charges, Bond Orders, and Bond Lengths of Selected States in Reaction 1 and Reaction 2 (4-31G)

atomic charge, bond order or bond length[b]	reaction 1				reaction 2	
	reactants	TS	product	Q[a]	reactant	product
$R(C-O_1)$	1.158	1.253	1.329		1.158	1.235
$B(C-O_1)$	0.470	0.290	0.176		0.470	0.432
$R(C-O_2)$	1.158	1.174	1.196		1.158	1.253
$B(C-O_2)$	0.470	0.480	0.518		0.470	0.387
$R(C-O_3)$	∞	1.575	1.349		∞	1.426
$B(C-O_3)$	0.0	0.005	0.167		0.0	0.118
$R(O_1-H_1)$	∞	1.35	0.953			
$B(O_1-H_1)$	0.0	0.119	0.259			
$R(O_3-H_1)$	0.950	1.119	2.246			
$B(O_3-H_1)$	0.265	0.119	0.002			
$Q(C)$	0.963	1.126	0.088	-	0.963	0.979
$Q(O_1)$	-0.482	-0.742	-0.706	+	-0.482	-0.759
$Q(O_2)$	-0.482	-0.541	-0.555		-0.482	-0.802
$Q(O_3)$	-0.804	-0.933	-0.555	+	-1.145	-0.788
$Q(H_1)$	0.402	0.593	0.457	-	0.145	0.371
$Q(H_2)$	0.402	0.490	0.459	-		

[a] Q is the sign of the external charge that when introduced around the atom could stabilize the reaction. [b] Bond length, $R(A-B)$, is in angstroms; bond order, $B(A-B)$, and atomic charge, $Q(A)$, are in electron charge.

Table VI. Energy Analysis of Reaction 2 (4-31G)

reaction coord $C-O_3$ (Å)	energy[a] (kcal/mol)				angle (deg)	
	$\Delta E_{DEF}(CO_2)$	$\Delta E_{DEF}(OH^-)$	$\Delta E(CO_2-OH^-)$	ΔE_{INT}	$\angle C-O_3-H_1$	$\angle O_1-C-O_2$
1.426	53.3	0.6	-82.6	-136.5	107.8	132.0
1.5	48.5	0.5	-81.4	-130.4	106.4	133.7
1.65	39.7	0.4	-73.9	-114.0	104.1	137.3
1.8	31.7	0.4	-64.1	-96.2	102.2	141.1
2.0	22.2	0.3	-51.6	-74.1	100.6	146.5
2.5	6.7	0.1	-29.3	-36.1	100.0	160.2
3.0	1.9	0.0	-17.5	-19.5	99.6	169.1

[a] ΔE_{INT}: interaction energy between deformed CO_2 and OH^-. Also see footnotes in Table III.

Table VII. Interaction Components in Reaction 2 (4-31G)

reaction coord $C-O_3$ (Å)	interaction energy[a] (kcal/mol)						charges transferred[b]
	ΔE_{INT}	ΔE_{MIX}	ΔE_{EX}	ΔE_{PL}	ΔE_{ES}	ΔE_{CT}	Q(CT)
1.426	−136.5	581.1	326.4	−77.6	−246.7	−719.7	−0.58
1.5	−130.4	452.2	257.3	−53.0	−204.5	−582.4	−0.56
1.65	−114.1	−20.9	156.3	−27.8	−140.0	−81.7	−0.52
1.8	−96.2	−23.0	93.4	−17.5	−96.9	−52.2	−0.46
2.0	−74.1	−15.5	46.2	−11.4	−61.7	−31.7	−0.37

[a] See footnotes in Table IV. [b] From OH^- to CO_2.

to reactants H_2O and CO_2 or product H_2CO_3 could be achieved by placement of external negative charge $-Q$ close to C, H_1, or H_2, and $+Q$ close to O_1 or O_3 in either direction. Also, a positive charge near O_2 will lower the barrier in the forward direction. Finally, the net charge transfer from H_2O to CO_2 is 0.15 electron in the transition state and 0.37 electron in the product (Table IV).

(2) Reaction 2. The one reaction coordinate is the $C-O_3$ distance, since we assume planar symmetry. Structures along the reaction pathway are optimized at the 4-31G level.

The energy analysis (Tables VI and VII) shows no barrier and yields a ΔE of formation of −82.6 kcal/mol in 4-31G, −60.3 kcal/mol in 4-31G+, and −40.0 kcal/mol in 4-31G+/MP2. The deformation energy of CO_2 is positive, increasing as OH^- approaches. Here, the angle O_1-C-O_2 is less deformed than it is in reaction 1. On the other hand, OH^- has almost no deformation energy (Table VI, third column). The large negative energy of interaction between deformed CO_2 and OH^- is so much larger in magnitude than the deformation energy that no barrier is found in the gas-phase reaction. Charge transfer and electrostatic interactions are larger in reaction 2 than in reaction 1, although polarization and exchange interactions are comparable (Table VII). At $C-O_3 \geq 1.5$ Å, $\Delta E_{ES} > \Delta E_{CT} > \Delta E_{PL}$, while at $C-O_3 < 1.5$ Å a large charge-transfer interaction accompanies formation of the $C-O_3$ bond.

Localized molecular orbitals change in a two-step fashion (Figure 4). Nucleophilic attack of O_3 on C to form $C-O_3$ bonding orbital (step a) is followed by simultaneous transformation of a bonding orbital on each of $C-O_1$ and $C-O_2$ into lone pairs on O_1 and O_2, respectively. Electron transfer occurs only in the OH^- to CO_2 direction throughout the reaction (Table V).

Geometric and population analyses (Table V) show that both $C-O_1$ and $C-O_2$ lengthen. The equilibrium bond distance of 1.426 Å for $C-O_3$ is comparable with results from other calculations.[26,27] Both O_3 and H become more positive and C, O_1, and O_2 become more negative as a total of 0.42 electron is transferred from OH^- to CO_2 when HCO_3^- is formed.

Discussion

Although PRDDO and STO-3G results for relative total energies, orbital eigenvalues, atomic charges, and dipole moments are in fair agreement,[28] reaction pathways present new problems. In electrophilic attack of OH^- on the carbonyl carbon of FCHO to give $FCH_2O_2^-$, the well depths[15] are 20 kcal/mol at OH^- to C of 2.01 Å with use of PRDDO and 17 kcal/mol at 2.25 Å with use of the 4-31G method. (Of course results for F^- attack are less satisfactory.) It is, however, known that the errors in PRDDO calculations are systematic, and that PRDDO preserves most of the qualitative properties, although the predicted energy barriers may be inaccurate. From the potential energy surface, we obtain here for reactions 1 and 2 (Methods section) barriers of 53 and 0 kcal/mol (4-31G), respectively, as compared with 52 and 0 kcal/mol obtained previously by others who used extended basis with limited CI.[9,10] Molecular geometries of the reactants, transition state, and product derived here are also similar to those obtained in other calculations.[9,10] Thus, PRDDO calculations

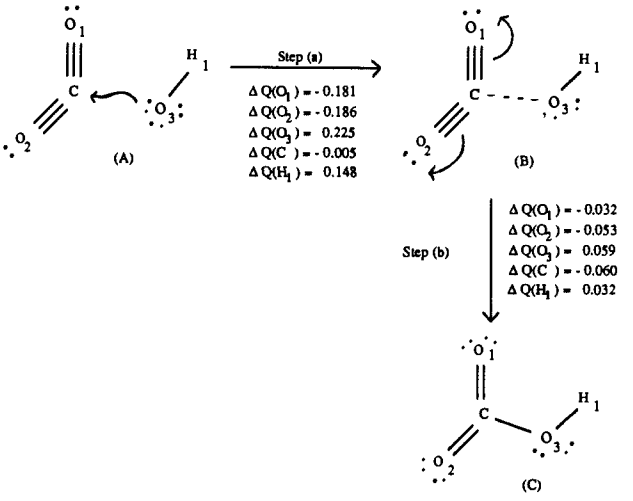

Figure 4. The sequence of electron flow for reaction 2. Step a: Nucleophilic attack of O_3 on C to form a $C-O_3$ bonding orbital. Step b: Simultaneous transformation of a bonding orbital on each of $C-O_1$ and $C-O_2$ into lone pairs on O_1 and O_2, respectively.

provide us a reasonable starting reaction energy surface, for which more complex calculations can be introduced to obtain accurate results. On the other hand, although the minumum basis SCF PRDDO approximation may give only an approximate pathway, the results from more extended basis sets and electron correlation at selected points of the pathway can be judged in part from Table II.

As H_2O approaches CO_2 at various orientations the relative flatness of the energy surface allows many pathways. Around the saddle point the energy remains within 3 kcal/mol of the PRDDO transition state for $1.55 \text{ Å} < C-O_3 < 1.7$ Å and $1.3 \text{ Å} < O_1-H_1 < 1.4$ Å. These values include transition states of other investigators[9-12] at different levels of calculations.

If only $C-O_3$ or O_1-H_1 is chosen as reaction coordinate a discontinuous jump in the other coordinate would be required, as illustrated, for example, by the o or x in Figure 2. Such an erroneous pathway and barrier can be avoided by inspecting at each discontinuity the secondary barrier, which is obtained by varying the second coordinate while the first is held constant. If a secondary barrier is found, more reaction coordinates are required to describe the reaction surface. Accordingly, we have examined all structural parameters at each point of the pathway: either there is no discontinuity, or there is no secondary barrier at a discontinuity such as that shown, for example, in step d of Figure 3.

In the Methods section we described a procedure for obtaining the MFRP step by step along the direction of least increase of energy. This procedure yields both the pathway and the transition state, while the step size can be adjusted for efficiency. The gradient method, used in earlier studies[29-31] to obtain the "minimum energy path" for other reactions, if applied here, would probably yield the same pathway, although one needs a structure

(26) George, P.; Bock, C. W.; Trachtman, M. *J. Comput. Chem.* **1982**, *3*, 283.
(27) Jönsson, B.; Karlström, G.; Wennerström, H. *J. Am. Chem. Soc.* **1978**, *100*, 1658.
(28) Halgren, T. A.; Kleier, D. A.; Hall, J. H.; Brown, L. D.; Lipscomb, W. N. *J. Am. Chem. Soc.* **1978**, *100*, 6595.
(29) Bender, C. F.; Pearson, P. K.; O'Neil, S. V.; Schaefer, H. F. *J. Chem. Phys.* **1972**, *56*, 4626.
(30) McIver, J. W.; Komornicki, A. *J. Am. Chem. Soc.* **1972**, *94*, 2625.
(31) Baskin, C. P.; Bender, C. F.; Bauschlicher, C. W., Jr.; Schaefer, H. F., III *J. Am. Chem. Soc.* **1974**, *96*, 2709.

of the transition state which is obtainable if a rough approximation to the pathway is known[31] (Appendix).

The reaction of CO_2 with H_2O (Table II, Figure 1) proceeds with concerted movements of O_3 to C and H_1 to O_1 before the transition state is reached, after which O_1–H_1 decreases faster than C–O_3. The deformation energies of CO_2 and H_2O are the major components of the barrier which could be lowered by placement of external charges around the deformed reactant molecules or by availability of vacant orbitals for sharing the crowded electron distribution. The positive interaction energies are also important: the exchange interaction, the most unfavorable one, could be stabilized in catalysis by adjacent vacant orbitals of comparable energy.

Although catalysis of these reactions is not studied here, some qualitative observations can be made. The population analysis (Table V) is suggestive that positive external charges around O_1 and O_3 and negative charges near atoms H_1, H_2, and C may reduce the energy barrier of the reaction of CO_2 with H_2O. However, the effects can be more complex as follows. (1) Both reactants and transition state can be stabilized, the latter more than the former. (2) Both reactants and transition state can be destabilized, the former more than the latter. (3) The transition state can be stabilized while the reactants are either destabilized or unaffected. (4) The reactants can be destabilized while the transition state is either stabilized or unaffected. In an earlier study[32] some effects of adjacent charges on the hydration of CO_2 have been evaluated with use of a special orientation between reactants and transition state. It was shown that unit positive charges around O_2 and around the hydrogens of H_2O are effective in lowering the energy barrier. Thus, a positive charge around O_2 is expected to decrease the repulsive energy between electrons on O_1 and O_2 as the angle O_1–C–O_2 decreases in the approach to the transition state, and the positive charges near both H_1 and H_2 (especially near H_1) destabilize both reactants and the transition state but the effects are larger on the reactants. Furthermore, a study of solvation effects[33] shows that when either OH^- or H_2O accepts a hydrogen bond from H_2 the barrier for hydration of CO_2 is lowered. Of course, the OH^- or H_2O helps to neutralize the positive charge that develops on H_2 as the transition state develops, but also the negative charges of additional OH^- or the electrons on additional H_2O may also facilitate the electron transfer of some 0.19 electron from H_2O to CO_2. Thus, either positive or negative charges near H_2, when placed at slightly different positions, can lower the barrier on the basis of different mechanisms. This somewhat complex behavior is probable sensitive to the relative orientation of these external charges, and thus charge placement (and movement) may be especially important in the active site of carbonic anhydrase.

The differences between reactions of CO_2 with H_2O (eq 1) and OH^- (eq 2) show (a) the absence of deformation energy of OH^- in reaction 2 and (b) the absence of a barrier in reaction 2 reflecting the stabilization by enhanced charge transfer and electrostatic interactions primarily due to the presence of a negative charge on OH^-. Also, in reaction 2 only one bond is formed, while in reaction 1 one bond is broken while two bonds are formed.

Solvent interactions play an important role in the barriers. The hydration reaction of reaction 1 has an experimental activation energy in solution of 17.7 kcal/mol[2] as compared with our theoretical value of 52.5 kcal/mol in the gas phase (Table II). For the reverse of reaction 1 the experimental activation energy in solution is 14.6 kcal/mol, while our calculated value (gas phase) is 46.4 kcal/mol (Table II). The reaction of CO_2 with OH^- (eq 2) has an experimental activation energy of 13.1 kcal/mol[2,3] in solution while our theoretical value is zero in the gas phase. If the effect of the enzyme is merely dehydration of reactant such that reaction 1 resembles the gas-phase reaction, the barrier would be raised by carbonic anhydrase. Actually, of course, the enzyme lowers the barrier largely by delivering OH^- to CO_2 at about pH 7 by greatly lowering the pK_a of the Zn^{2+}-bound water molecule.

Use of water monomer for the gas-phase hydration of CO_2 in a four-membered ring transition state gives a high barrier of 52.5 kcal/mol, which is typically 38 to 68 kcal/mol in comparable bimolecular reactions.[11,34-36] However, the use of a hydrogen-bonded water dimer reduces the barrier by some 26–46 kcal/mol.[11,34-36] In particular the barrier for hydration of CO_2 by water dimer in the six-membered ring configuration is lowered by 26 kcal/mol at the 3-21G level.[11] In the reaction of OH^- no proton transfer is required, and the appearance of the barrier in solution may be associated with displacement of water from hydration stabilized OH^-; here the transition state appears not to be stabilized by hydration as much as are the reactants and product.

In studies of other bimolecular reactions, in which both nucleophilic attack of O (or N) on C and proton transfer within a four- or five-membered ring occur, the molecular deformation energy amounts to 20% to 103% of the barrier.[34,36,37] In these other studies C–O (or C–N) bond lengths in these transition states range from 1.565 to 1.674 Å, and proton transfer has hardly begun. In our study, reaction 1 has a very high deformation energy owing to O···O repulsion in CO_2 and to proton transfer further in the transition state.

Because the transition state for reaction 1 involves some delocalization of valence orbitals, correlation corrections are expected to be of some importance. We find that addition of polarization functions to all atoms in the 4-31G basis yielding a 4-31G** basis raises the barrier of reaction 1 by about 10 kcal/mol and that correlation to give a 4-31G**/MP2 basis lowers the barrier by about this same amount (Table II). While errors associated with neglect of polarization and correlation corrections in isoelectronic closed shell neutral systems are sometimes small,[38,39] and a 4-31G basis may give good results,[40] no general conclusion that the 4-31G basis is adequate can be drawn. In addition, inclusion of diffuse orbitals on the heavy atoms, thus transforming the 4-31G basis to the 4-31G+ basis, raises the barrier of reaction 1 by 2.5 kcal/mol, while the reaction energy of reaction 2 is increased significantly from −83 kcal/mol in the 4-31G basis, to −60 kcal/mol in the 4-31G† basis, and to −40 kcal/mol in the 4-31G**/MP2 basis (Table II), primarily due to negative charges of the anions, OH^- and HCO_3^-.

In the remainder of this discussion we consider corrections to the ab initio barrier ΔE_0 arising from zero-point vibrations (ΔZPV) and finite temperature T (Δthermal) assuming ideal gas behavior to give an estimate of ΔE_T^+. Vibrational frequencies are estimated by using the Gaussian 82 program at each stationary state. The standard formulas for partition functions are then used,[41] from which we obtain ΔZPV as 0.13 kcal/mol and Δthermal as −0.99 kcal/mol at 25 °C. Most of this latter number arises from translatonal energy ($-1.5RT$). Thus, $\Delta E_T^+ = \Delta E$ + ΔZPV + Δthermal is 52.5 kcal/mol at the 4-31G level, and 51.6 kcal/mol when the 4-31G optimized geometry is used at the 4-31G**/MP2 level. The activation enthalpy is 51.9 and 51.0 kcal/mol at these two levels, following the ΔPV correction.

The activation entropy ΔS_T^+ is −32.2 cal/(mol·K) of which −33.6, −1.1, and 2.5 cal/(mol·K) are translational, rotational, and vibrational contributions, respectively. Thus ΔG_T^+ is 61.5 kcal/mol at the 4-31G level and 60.7 kcal/mol at the 4-31G**/MP2 level at 25 °C. The entropic contribution is therefore about 15% of the total.

We estimate that discrepancies between calculated and observed vibrational frequencies cause an error of less than 2 kcal/mol on

(32) Sokalski, W. A. *Int. J. Quantum Chem.* **1981**, *20*, 231.
(33) Sokalski, W. A.; Sawaryu, A.; Chojnacki, H. *Int. J. Quantum Chem., Quantum Biol. Symp.* **1983**, *10*, 321.
(34) Williams, I. H.; Spangler, D.; Femec, D. A.; Maggiorn, G. M.; Schowen, R. L. *J. Am. Chem. Soc.* **1983**, *105*, 31.
(35) Oie, T.; Loew, G. H.; Burt, S. K.; Binkley, J. S.; MacElroy, R. D. *J. Am. Chem. Soc.* **1982**, *104*, 6169.
(36) Nguyen, M. T.; Hegarty, A. F. *J. Am. Chem. Soc.* **1983**, *105*, 3811.
(37) Nguyen, M. T.; Sana, M.; Leroy, G.; Dignam, K. J.; Hegarty, A. F. *J. Am. Chem. Soc.* **1980**, *102*, 573.
(38) Dedieu, A.; Veillard, A. *J. Am. Chem. Soc.* **1972**, *94*, 6730.
(39) Benson, M. J.; McLaughlin, D. R. *J. Chem. Phys.* **1972**, *56*, 1322.
(40) Szczesniak, M. M.; Scheiner, S. *J. Chem. Phys.* **1982**, *77*, 4586.
(41) Rice, O. K. *Statistical Mechanics, Thermodynamics and Kinetics*; W. H. Freeman and Company: San Francisco, 1967.

the basis of comparisons for H_2O, HCO_3^-, and CO_2.[26,42] Also, errors in $-T\Delta S_T^+$ are probably small ($\leq$1 kcal/mol) because of the small contributions ($\sim$4%) of the most uncertain terms (vibrational and rotational). Thus, the errors in the thermodynamic contributions to the free energy are about 2–3 kcal/mol.

We also find that the 4-31G and 4-31G+ bases yield similar values (differing by less than 0.5 kcal/mol) for ΔZPV, Δthermal, and ΔS_T^+. Thus, the differences in ΔE_T^+ and ΔG_T^+ reside mostly in the value of ΔE_0. At the 4-31G+ level ΔE_T^+, ΔS_T^+, and ΔG_T^+ of reaction 1 are 55.5 kcal/mol, −32.5 cal/(mol·K) and 64.6 kcal/mol, respectively (Table II).

In addition, the heat of formation of H_2CO_3 from H_2O and CO_2 is −1.7 kcal/mol (4-31G), 4.4 kcal/mol (4-31G**), 9.2 kcal/mol (4-31G**/MP2), 1.1 kcal/mol (4-31G+), and 16.4 kcal/mol (4-31G+/MP2), while the experimental value is 4.8 kcal/mol at 298 K.[26] Also, the heat of formation of HCO_3^- from OH^- and CO_2 is −79.3 kcal/mol (4-31G), −57.2 kcal/mol (4-31G+), and −36.9 kcal/mol (4-31G+/MP2), while the experimental value is ca. −49 kcal/mol at 298 K.[43,44]

Acknowledgment. We thank the National Science Foundation (Grant CHE-82-10536) for support of this research and for an initial grant to the Computer Center (Grant PCM-77-11398).

Appendix

The minimum energy path is the gradient curve on the energy surface that connects the transition state with the states of the reactants and the product. To obtain the gradient curve, one starts from the transition state, moves along the direction of the only negative eigenvalue of the force constant matrix at the transition state, and then follows the gradient direction at each point, which in one direction leads to the reactants and in the other to the product. To show that the minimum energy path thus obtained is equivalent to the most favorable reaction pathway obtained here, we will consider the two-dimensional potential function $V(x,y) = xy$ as an example, which has a saddle point at $x = y = 0$. The contour map of $V(x,y)$ is shown in the following figure, where V equals zero on both the x and y axes, the $V(x,y) = C$ curves in the first and third (second and fourth) quadrants are pairs of hyperbolas of positive (negative) C values with the value C increasing (decreasing) as the curve moving away from the origin.

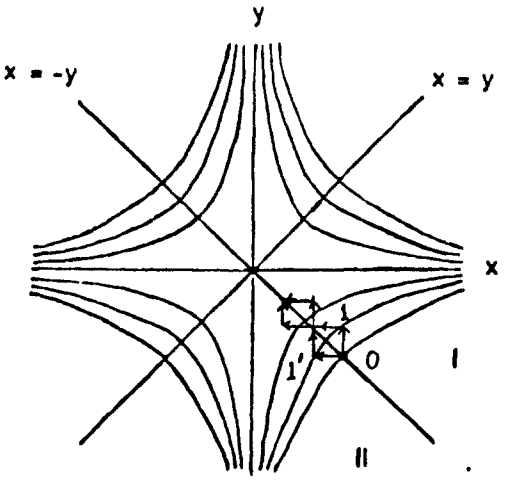

The minimum energy path in this example is simply the line $x = -y$, passing through the second and the fourth quadrants, connecting the origin (the transition state) with point $(-\infty, \infty)$ (the product) and point $(\infty, -\infty)$ (the reactants). To construct the most favorable reaction pathway, only the fourth quadrant of the contour map will be considered here (since the second quardant is its mirror image through the line $x = y$). The fourth quadrant can be further divided into two halves, region I and region II, by the line $x = -y$. The gradient $(g_x, g_y) = (y, x)$ evaluated inside region I will always have a larger y component ($|g_y| = |x| > |y| = |g_x|$), while those evaluated inside region II have a larger x component ($|g_x| > |g_y|$); and for those points sitting on line $x = y$, g_x is equal to g_y. If we start with any point on line $x = -y$ in the 4th quadrant, since $|g_x| = |g_y|$, the curve can proceed along either the y axis going upward or the x axis going leftward. Suppose the upward movement to point 1 in region I is selected, since $|g_x| < |g_y|$ at any point in region I, the curve will move leftward, which pulls the path back toward the central line $x = -y$. On the other hand, if previously the leftward movement to point 1′ is chosen, since $|g_y| < |g_x|$ in region II, the curve will move upward, and thus will also pull the path back toward the $x = -y$ line. Accordingly, the resultant pathway will be a curve winding around the minimum energy path $x = -y$; and when the step size of each consecutive movement is reduced toward zero, the limiting pathway will coincide with the minimum energy path. Finally, if any point other than those on the $x = -y$ line is chosen as the starting point, the first few steps will be either consecutively moving leftward or moving upward until the path is carried far enough to merge with the line $x = -y$, i.e., the minimum energy path.

Registry No. CO_2, 124-38-9; H_2O, 7732-18-5; OH^-, 14280-30-9.

(42) Silverstein, R. M.; Bassier, G. C.; Morrill, T. C. *Spectrometric Indentification of Organic Compounds*; John Wiley & Sons: New York, 1981; p 96.

(43) The heat of reaction for $CO_2 + OH^- \rightarrow HCO_3^-$ in the gas phase is obtained by the equation $\Delta H = [\Delta H_f(H_2CO_3)_g - \Delta H_f(CO_2)_g - \Delta H_f(H_2O)_g]$ + (proton affinity of OH^-) − (proton affinity of HCO_3^-), where $\Delta H_f(H_2CO_3)_g = -147$ kcal/mol, $\Delta H_f(CO_2)_g = -94$ kcal/mol, and $\Delta H_f(H_2O)_g = -58$ kcal/mol;[26,44] the proton affinity of OH^- is 391 kcal/mol,[17] and the proton affinity of HCO_3^- is 337 ± 3 kcal/mol (estimated from the 4-31G+ calculations).

(44) Pedley, J. B.; Rylance, J. *Sussex-NPL computer analysed thermodynamical data: Organic and Organometallic Compounds*; Universty of Sussex: England, 1977.